

# Laboratory and Field Evaluation of a New Personal Sampling System for Assessing the Protection Provided by the N95 Filtering Facepiece Respirators against Particles

SHU-AN LEE<sup>1</sup>, SERGEY A. GRINSHPUN<sup>1</sup>, ATIN ADHIKARI<sup>1</sup>, WEIXIN LI<sup>1</sup>, ROY MCKAY<sup>1</sup>, ANDREW MAYNARD<sup>2</sup> and TIINA REPONEN<sup>1\*</sup>

<sup>1</sup>Department of Environmental Health, University of Cincinnati, P.O. Box 670056, Cincinnati, OH 45267-0056, USA; <sup>2</sup>Centers for Disease Control and Prevention, National Institute for Occupational Safety and Health, 4676 Columbia Parkway, Cincinnati, OH 45226, USA

Received 25 May 2004; in final form 14 September 2004; published online 24 January 2005

**Objectives:** We have recently developed a new personal sampling system for the real-time measurement of the protection provided by respirators against airborne dust and micro-organisms. The objective of this study was to evaluate the performance characteristics of the new sampling system in both laboratory and field conditions.

**Methods:** The measurements were conducted using the N95 filtering facepiece respirators and the newly developed personal sampling system put on a manikin (laboratory study) or donned by a human subject (laboratory and field studies). Two inhalation flow rates (0 and 40 l min<sup>-1</sup>) in conjunction with the sampling flow rate (10 l min<sup>-1</sup>) were tested in the manikin-based experiments to investigate the effects of the leak location (nose, cheek and chin) and the depth of the sampling probe (0, 5, 10 and 15 mm) within the respirator. The effect of human activity on the protection factor was evaluated using a variety of head movements and breathing patterns when a human subject wore the respirator in a room-size laboratory test chamber. The field study was conducted during corn harvesting with a respirator worn by a human subject on a combine.

**Results:** There was no significant difference in the protection factors for different leak locations, or for sampling probe depths, when the inhalation rate was 0 l min<sup>-1</sup>. For the inhalation rate of 40 l min<sup>-1</sup>, the protection factors for nose leaks were higher than those for chin and cheek leaks. Furthermore, the protection factor was the lowest and showed the least variation when the sampling probe depth was equal to 0 mm (imbedded on the respirator surface). Human subject testing showed that the grimace maneuver decreased the protection factor and changed the original respirator fit. The protection factor during breath holding was lower than that found during inhalation and exhalation. Field results showed greater variation than laboratory results.

**Conclusions:** The newly designed personal sampling system efficiently detected the changes in protection factors in real time. The sampling flow was least affected by the inhalation flow when the sampling probe was imbedded on the respirator surface. Leak location, breathing patterns and exercises did affect the measurement of the protection factors obtained using an N95 filtering facepiece respirator. This can be attributed to the differences in the in-mask airflow dynamics contributed by the leak, filter material, sampling probe and inhalation. In future studies, it would be beneficial if the laboratory data could be integrated with the field database.

**Keywords:** breathing pattern; depth of the sampling probe; fit testing; leak location; leak size; protection factor; respirator

## INTRODUCTION

Respirators are generally used to protect people from air contaminants entering the human body through the respiratory tract. Among the various types of

\*Author to whom correspondence should be addressed.  
Tel: +1-513-558-0571; fax: +1-513-558-2263;  
e-mail: reponeta@ucmail.uc.edu

respirators, the N95 filtering facepiece respirators (one type of air purifying respirator) are widely used. The Centers for Disease Control and Prevention (CDC) has recommended the use of these respirators by health care workers to protect them from infectious aerosols, which can cause diseases such as tuberculosis and severe acute respiratory syndrome. The number '95' in this designation indicates that the filtration efficiency of the respirator is at least 95% at the most penetrative particle size of 0.3  $\mu\text{m}$ . The letter 'N' indicates that this type of respirator is not resistant to oil (CDC, 1995). Qian *et al.* (1998) found that the filtration efficiency of the N95 respirators is 99.5% or higher for particles in the size range of bacteria (aerodynamic diameter > 0.75  $\mu\text{m}$ ).

The protection provided by a respirator is represented by the protection factor, which is defined as the ratio of the contaminant concentration outside the respirator to the contaminant concentration inside. Thus, for a specific contaminant, the protection factor is the inverse of the penetration efficiency. Air contaminants can enter the respirator cavity through the filter material, face-seal leaks and other inward leaks caused by damage or other defects. Thus, the concentration of air contaminants inside the respirator is the sum of the concentrations of the contaminants entering through the different pathways. When the respirator is used in accordance with a properly administered respiratory protection program, inward leaks are minimized.

Several studies have evaluated the factors that can affect the respiratory protection against airborne particles, such as leak location, leak shape, leak size, respirator type, facial dimension, particle shape, particle size, inhalation rate and inhalation resistance (Chen *et al.*, 1990, 1992; Willeke *et al.*, 1996; Crutchfield *et al.*, 1997; Brazile *et al.*, 1998; Qian *et al.*, 1998; Nelson *et al.*, 2000). After the aerosol particles penetrate through the leak, the aerosol measurement inside the respirator is affected by the spatial variation of the particle concentration and the particle size distribution in the mask cavity, as well as by the breathing pattern, lung retention (Hewett *et al.*, 1993; Hinds *et al.*, 1993) and sampling losses inside the respirator (Liu *et al.*, 1984; Holton *et al.*, 1987). The concentration inside the respirator is measured by a sampling probe. Various probe locations have been evaluated with different face-seal leak sites and different breathing patterns (Myers *et al.*, 1988). A sampling bias has been identified and has been shown to depend on the probe location (Myers *et al.*, 1988), the probe depth inside the facepiece (Myers *et al.*, 1988) and the sampling method (continuous flow versus pulse flow) (Coffey *et al.*, 1998). The research on sampling bias has focused on vaporous test agents (Myers *et al.*, 1988), and more work is needed for evaluating the sampling bias with particulate contaminants. In addition, most of the

previous studies were done under laboratory conditions. Thus, it is important to evaluate how the laboratory-generated data reflect the workplace conditions.

We have recently developed a new personal sampling system (Lee *et al.*, 2004) to determine the protection provided by respirators against biological and non-biological particles. Using this sampling system, the particle concentration of five particle size fractions can be measured in real time within a range of 0.7–10  $\mu\text{m}$  inside and outside the respirator when a worker wears the respirator during his/her usual work activities. The protection factor can be determined with this system in both the laboratory and field test conditions.

Our previous paper (Lee *et al.*, 2004) describes the development and optimization of the prototype of the newly developed personal sampling system. This paper presents the laboratory and field evaluations of this sampling system. The objectives of this study were to determine: (i) how well the new sampling system detects protection factors in real time; and (ii) whether the leak locations, the depths of the sampling probe, human activity and breathing patterns affect the measurement of the protection factor as a function of particle size. Laboratory measurements of the protection factor were made over a range of simulated leak locations and depths of the sampling probe, while an N95 filtering facepiece respirator was put on a manikin head and operated at two inhalation flow rates. In addition, the effects of different head movements and breathing patterns on protection factors were evaluated with a human subject. Finally, field testing was performed using a human subject working in a cornfield.

## MATERIALS AND METHODS

The particle concentrations outside and inside the N95 respirator were measured using our newly developed personal sampling system (Lee *et al.*, 2004). The sampling system was either put on a manikin or donned by a human subject wearing an N95 facepiece respirator (Model 8210; 3M, St. Paul, MN, USA). Figure 1 shows a schematic representation of the sampling system used in the manikin-based experiments in this study. The real-time concentration was monitored by an optical particle counter (OPC; Model HHPC-6, ARTI Inc., Grants Pass, OR, USA) for five particle size fractions: 0.7–1, 1–2, 2–3, 3–5 and 5–10  $\mu\text{m}$ . When testing for airborne microorganisms, the samples were also collected on a filter sampler. The protection provided by the N95 filtering facepiece respirator was initially assessed by performing experiments with a manikin head using artificial leaks and later with a human subject having natural face-seal leaks. All human subject experiments in this study were performed on the same individual.

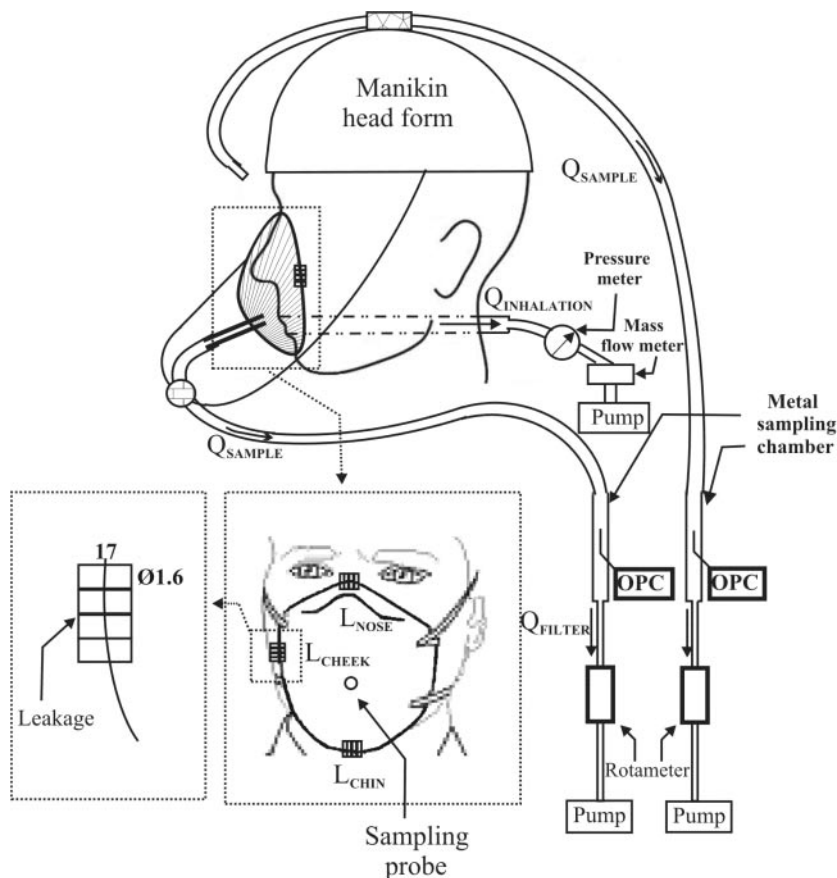


Fig. 1. Schematic representation of the personal sampling system used in the manikin-based testing.

### Laboratory test environment

A walk-in indoor test chamber ( $860 \text{ ft}^3 = 24.3 \text{ m}^3$ ) developed in the Center for Health-Related Aerosol Studies (University of Cincinnati) and used in our previous investigations (Choe *et al.*, 2000; Grinshpun *et al.*, 2004) was utilized to conduct the laboratory testing for this study. The test chamber was maintained at a positive pressure of 1 in. w.g. (249 Pa) during the experiments. Sodium chloride solution (NaCl, 1%, w/v) was aerosolized in the chamber by a six-hole Collison nebulizer (BGI Inc., Waltham, MA, USA) at a pressure of 20 psi ( $1.38 \times 10^5 \text{ Pa}$ ) and a flow rate of  $12 \text{ l min}^{-1}$ . Dry air was mixed with NaCl aerosols at a flow rate of  $40 \text{ l min}^{-1}$ . NaCl was used as a primary test aerosol at concentrations ranging from  $4.2 \times 10^7$  to  $1.9 \times 10^8 \text{ particles m}^{-3}$ . As the number concentrations of the larger NaCl particles ( $5\text{--}10 \mu\text{m}$ ) generated by the Collison nebulizer were not sufficient for 1-min measurements, Arizona road dust dispersed by a cyclonic vacuum cleaner (Bagless Cyclonic System, Model 4481, EUREKA Company, Bloomington, IL, USA) was used as a test aerosol to represent larger particle sizes when comparing the penetration of particles through the sampling system with and without the installation of a dryer. The dryer

was used to remove water from human-exhaled air as described below. The aerosol concentrations of Arizona road dust ranged from  $5.3 \times 10^7$  to  $7.5 \times 10^7 \text{ particles m}^{-3}$ . Since laboratory-generated particles may carry high electrical charges, the entire airflow of  $52 \text{ l min}^{-1}$  was directed through a 10 mCi  $^{85}\text{Kr}$  charge equilibrators (Model 3054, TSI, Inc., Minneapolis, MN, USA) to achieve the Boltzmann charge equilibrium. An air circulation fan (with a flow rate of  $\sim 900 \text{ CFM}$ ) located at the outlet of the aerosol generation system distributed the aerosolized particles within the chamber.

### Leak location and the depth of the sampling probe

Fixed-size leaks were created for each leak location using four circular copper tubes. To achieve sufficient particle concentration inside the respirator (which was a challenge, especially for the particles  $>0.7 \mu\text{m}$ ), the minimum leak was chosen to have a single cylindrical copper tube with a diameter of 1.6 mm (cross-section area of  $2 \text{ mm}^2$ ). All tubes had a length of 17 mm. Three locations were established for the fixed-size leaks: at the left side of the bridge of the nose ( $L_{NOSE}$ ), the left cheek ( $L_{CHEEK}$ ) and chin ( $L_{CHIN}$ ) (Fig. 1). For these three locations, the leaks were

positioned/glued along the sealing edge of the respirator ~60 mm from the in-facepiece sampling probe, which was imbedded on the respirator surface opposite to the mouth. Because the cheek is not flat and has a slope, the leaks were positioned at an angle, which was naturally formed by the cheek and the outer surface of the respirator.

The experiments at different leak locations were conducted by closing or opening specific copper tubes with stoppers. Generally, there were two airflows inside the respirator during the test representing the flow through the in-facepiece sampling probe ( $Q_{\text{SAMPLE}}$ ) and inhalation flow ( $Q_{\text{INHALATION}}$ ) (Fig. 1). Each test was performed at  $Q_{\text{INHALATION}} = 0$  and  $40 \text{ l min}^{-1}$ . To introduce the inhalation airflow into the respirator cavity, copper tubing (inner diameter = 1 in.  $\approx 25.4 \text{ mm}$ ; length = 170 mm) was inserted straight from the back to the mouth of the manikin head. The inhalation flow was monitored by a thermal mass flow meter (Model 4043, TSI, Inc., Minneapolis, MN, USA). The pressure drop through the filter material and leaks was measured by a pressure meter (Magnehelic, Dwyer Instruments Inc., Michigan City, IN, USA) positioned behind the manikin's head. Measurements on the particle penetration through the filter material were performed with the respirator tightly sealed to the manikin's face with no artificial leakage.

The manikin's head was positioned at the center of the test chamber at a height of 1 m from the floor. An N95 filtering facepiece respirator was glued to the manikin's face with a silicone sealant (GE Sealants and Adhesives, Huntersville, NC, USA). The effect of the leak location on the protection factor was tested with a leak size of  $2 \text{ mm}^2$  at these different leak locations. The effect of the sampling probe depth was assessed at depths of 0, 5, 10 and 15 mm away from the respirator surface with a  $2 \text{ mm}^2$  leak located at the chin. The respective distances from the inlet of the sampling probe to the mouth were 19, 14, 9 and 4 mm.

#### *Dryer designed for human experiments*

Human-exhaled air, saturated with water vapor often causes instrumental dysfunction that may bias or even prevent measurement of particle concentrations. In addition, high humidity may change the particle size distribution inside the respirator due to condensation and hygroscopic growth. Thus, removing water vapor from the exhaled air without altering the concentration of the particles is very important for accurate particle size selective measurements.

Silica gel is widely used as an air desiccant. For example, a common laboratory diffusion dryer, such as TSI-Model 3062 (TSI Inc., Shoreview, MN, USA), utilizes silica gel. However, this type of dryer is usually only suitable for stationary applications, because silica gel may release small particles if the unit

is moved or disturbed. In contrast, Nafion tubing (Perma Pure Inc., Toms River, NJ, USA), which has been used in aerosol dryers in several studies (Day *et al.*, 2000; Ojanen *et al.*, 2004), does not generate additional particles under similar circumstances. In addition, Nafion is only permeable to water and the equilibrium is reached very quickly so that water removal from the sample air stream is completed in 100–200 ms. Water passes through the Nafion tubing from a high-humidity environment to a low-humidity environment until an equilibrium is reached.

To remove water efficiently from the exhaled air using the Nafion tubing, a sufficient humidity gradient should be maintained. In commercially available Nafion dryers (e.g. Models PD-50T, PD-100T and PD-200T), this is achieved by directing the sampling airflow through several parallel Nafion tubes and a separate dry airflow through the dryer outside the Nafion tubes. The efficiency of the dryer depends on the humidity and the amount of flow. For efficient drying, it is recommended that the drying airflow should be 2–3 times the sampling flow. In our sampling system, the sampling flow of  $10 \text{ l min}^{-1}$  requires a drying airflow of  $20\text{--}30 \text{ l min}^{-1}$ , which is not feasible for personal sampling.

To make a dryer that is portable and suitable for the field test, we combined the principles of the silica gel and Nafion dryers. A bundle of 12 Nafion tubings (0.11 in.  $\approx 2.8 \text{ mm}$  outer diameter and 5 in.  $\approx 127 \text{ mm}$  length) was placed inside a plastic cylinder (1.5 in.  $\approx 38 \text{ mm}$  diameter and 5 in.  $\approx 127 \text{ mm}$  length). The silica gel (Fisher Scientific, Pittsburgh, PA, USA) was placed between the inner layer of the plastic cylinder and the outer layers of 12 Nafion tubings. When the silica gel is saturated with water, its indicator (chloride cobalt) changes color from blue to pink indicating that it must be replaced. In our field study, we found that the silica gel maintained a sufficiently low humidity for 3–4 h before it had to be replenished. The total weight of the dryer was  $\sim 100 \text{ g}$  and it did not require any additional airflow. Thus, the combination of silica gel and Nafion tubing was found ideally suited for field use.

#### *Particle losses*

The particle losses in the sampling line have been addressed in our previous study (Lee *et al.*, 2004). We found a difference in the penetration efficiencies of particles between the two sampling lines due to slightly different configurations as well as the counting efficiencies of the two OPCs. Therefore, all the protection factors presented in this paper were corrected by a ratio of the concentrations measured in the two sampling lines.

#### *Human activity and breathing patterns*

The effect of human activity and breathing patterns on protection factors was assessed using a human



subject wearing an N95 filtering facepiece respirator. Before the experiment started, the subject was required to pass the quantitative fit testing conducted with a TSI Portacount Plus in combination with N95 companion (TSI, Inc., St. Paul, MN, USA). A fit factor (FF) of 100 or above was considered an acceptable passing value. In order to investigate the effect of human activity on the protection factor, fit-testing exercises were performed according to the OSHA fit-testing protocol specified in 1910.134. These exercises include normal breathing, deep breathing, turning the head from side to side, moving the head up and down, talking, grimace maneuver, bending over and touching the toes, and returning to normal breathing (US Department of Labor, 1998). Each exercise was performed for 2 min and the particle concentrations inside and outside the respirator were averaged over 1-min periods.

The effect of breathing patterns on the protection factor was investigated in two different experiments. First, a series of consecutive manipulated breathing patterns were performed: breath holding, inhalation, breath holding, exhalation, breath holding, inhalation, breath holding, exhalation and returning back to breath holding. Each breathing pattern was performed for 6 s. The particle concentrations inside and outside the respirator were measured continuously during this test and averaged over 6-s intervals. The test was repeated three times with a 1-min rest time between repeats. The protection factor for each breathing pattern was calculated by averaging the data from all three repeats. Second, a separate experiment was performed when a subject breathed normally sitting in the indoor test chamber for 9 min with particle concentrations recorded continuously with 6-s averages.

#### Field test

The corn-harvesting site was located in an open cornfield at Clarksville, OH, USA. The average of the total particle concentration measured with the OPC in the size range of 0.7–10  $\mu\text{m}$  was  $3 \times 10^8$  particles  $\text{m}^{-3}$ , which was about the same as the concentration generated in the laboratory. The field test was conducted when a farmer was driving a combine during corn harvesting. A human subject wearing a respirator stood on the combine, outside the cockpit, in order to collect sufficient particle concentrations inside the respirator. The measurements were conducted continuously for 30 min with particle concentrations averaged over 1-min periods.

#### Data analysis

Data analysis was performed using a repeated measurement linear model using the Statistical Analysis System (SAS) version 8.0 (SAS Institute Inc., Cary, NC, USA).  $P$ -values of  $<0.05$  were considered significant. The independent variables

in the model were the leak location, the depth of the sampling probe, the inhalation rate and the particle size. The dependent variable was the protection factor. Since the protection factors obtained at different depths of the sampling probe were not normally distributed (as required by the assumption of the model), the data were inversed to achieve the normality. The repeated measurement linear model analysis was performed using the PROC MIX program statements while the PROC UNIVARIATE program statement was used for the normality tests.

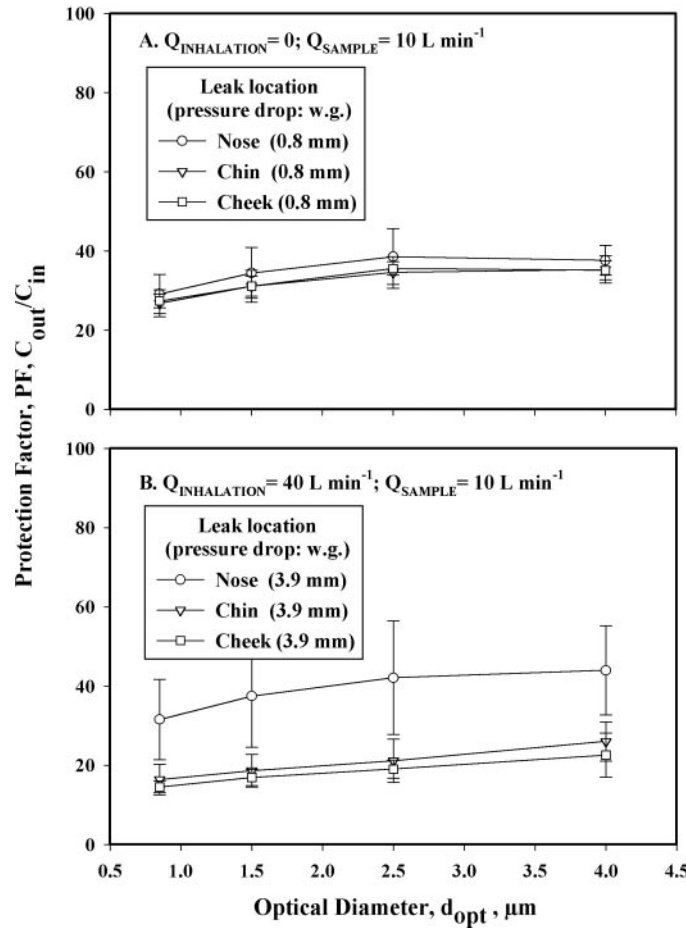
## RESULTS AND DISCUSSION

Figure 2A and B shows the effect of the leak location on the protection factor of an N95 respirator for different particle sizes. Figure 2A presents the results obtained at the total flow of  $10 \text{ l min}^{-1}$  ( $Q_{\text{INHALATION}} = 0.1 \text{ min}^{-1}$ ;  $Q_{\text{SAMPLING}} = 10 \text{ l min}^{-1}$ ) while Fig. 2B presents the results for the total flow of  $50 \text{ l min}^{-1}$  ( $Q_{\text{INHALATION}} = 40 \text{ l min}^{-1}$ ;  $Q_{\text{SAMPLING}} = 10 \text{ l min}^{-1}$ ). Each curve represents a specific leak location (nose, cheek and chin). The protection factor provided by the N95 filtering facepiece respirator varied from 10 to 44, depending on the leak location, the inhalation flow rate and the particle size. For the particle size range of 0.7–5  $\mu\text{m}$ , the protection factor was found to be 143 or greater at the inhalation rate of  $40 \text{ l min}^{-1}$  when the respirator was sealed on the manikin's face without artificial leakage. This factor is 3–14 times greater than that obtained for a 2  $\text{mm}^2$  artificial leak. Therefore, most of the aerosol inside the respirator penetrated through the leaks.

There was no significant effect of the leak location on the protection factor ( $P > 0.05$ ) when no inhalation flow was established (the only flow rate inside the respirator was  $Q_{\text{SAMPLE}}$ ) (Fig. 2A). In contrast, there was a significant difference in the protection factors obtained for the different leak locations ( $P < 0.05$ ) that occurred when the inhalation rate was increased to  $40 \text{ l min}^{-1}$  (Fig. 2B). In this case, the highest protection factor was found when the leak was located at the manikin's nose. As the aerosol concentration outside the respirator remained constant, the higher protection factor corresponds to a lower concentration inside the respirator. This can be explained by the increased velocity through the leak and the airflow dynamics inside the respirator. When the inhalation rate was increased from 0 to  $40 \text{ l min}^{-1}$ , the pressure drop increased from 0.8 to 3.9  $\text{mm w.g.}$  Information on the pressure drop can be used to calculate the leak flow,  $Q_{\text{LEAK}}$  ( $\text{l min}^{-1}$ ) as follows (Chen *et al.*, 1992):

$$Q_{\text{LEAK}} = Q_{\text{TOTAL}} \times \frac{|\Delta P_{\text{LEAK}} - \Delta P_{\text{SEAL}}|}{\Delta P_{\text{SEAL}}} \quad (1)$$

where  $\Delta P_{\text{LEAK}}$  ( $\text{mm w.g.}$ ) is the pressure drop measured with the leak,  $\Delta P_{\text{SEAL}}$  ( $\text{mm w.g.}$ ) is the pressure drop measured without the leak and  $Q_{\text{TOTAL}}$



**Fig. 2.** Effect of the leak location on the protection factor at two inhalation flow rates: (A) 0 and (B) 40 l min<sup>-1</sup>. The tests were performed using NaCl aerosol. The N95 respirator was fitted to the manikin's head. The leak cross section = 1 × 2 mm<sup>2</sup>; depth of the sampling probe = 0. Each data point represents an average and standard deviation of three repeats. Each repeat was done with the same type of unused respirator.

(l min<sup>-1</sup>) is the total flow rate coming into the respirator cavity (through the filter and the leak). The velocity of the leak flow,  $V_{LEAK}$  (m s<sup>-1</sup>), was calculated as follows (ACGIH, 1998):

$$V_{LEAK} = \frac{Q_{LEAK}}{A_{LEAK}} \times 16.67 \quad (2)$$

where  $A_{LEAK}$  (mm<sup>2</sup>) is the total leak area and 16.67 is a unit conversion factor. At  $Q_{TOTAL} = Q_{SAMPLE} + Q_{INHALATION} = 50 \text{ l min}^{-1}$ ,  $\Delta P_{LEAK}$  was 3.9 mm w.g. and  $\Delta P_{SEAL}$  was 4.1 mm w.g. Thus, the leak flow and the velocity for the 2 mm<sup>2</sup> leak at this condition were calculated to be 2.4 l min<sup>-1</sup> and 20.4 m s<sup>-1</sup>, respectively.

At an air jet velocity from the leak into the respirator cavity as high as 20.4 m s<sup>-1</sup>, the leak flow regime, which was laminar (Chen *et al.*, 1992) at  $Q_{TOTAL} = Q_{SAMPLE} = 10 \text{ l min}^{-1}$ , became transitional (between laminar and turbulent) at  $Q_{TOTAL} = 50 \text{ l min}^{-1}$  (Re = 2171) (Baron *et al.*, 2001). When the leak occurred at the cheek or chin, the air jet was directed toward the sampling probe, where the leak flow mixed well with

the sampling flow. The velocity at the inlet of the sampling probe was 20.7 m s<sup>-1</sup>, which was calculated by dividing the sampling flow ( $Q_{SAMPLE}$ ) by the area at the inlet of the sampling probe (ACGIH, 1998). For the nose leak, the jet of the same initial velocity was directed toward the respirator filter located 30 mm away from the leak. The terminal velocities were calculated based on the ASHRAE formula for the centerline velocity of the throw of nozzle jets (ASHRAE, 1997). This jet flow reached the respirator filter at a terminal velocity of 12.4 m s<sup>-1</sup>, resulting in particle losses due to the impaction on the respirator filter fibers. In addition, the nose bridge restricted directing the jet flow to the sampling probe and redirected it to the side of the respirator, which led to poor mixing between the nose leak flow and the sampling flow. Besides, the particle losses due to the impaction on the nose bridge also contributed to the decreased aerosol particles sampled by the sampling probe. Therefore, the aerosol concentration was higher when the leak occurred at the cheek or chin than when it occurred near the nose.

When the inhalation rate was increased from 0 to  $40 \text{ l min}^{-1}$ , the protection factors measured with the leaks located at the chin and cheek decreased significantly ( $P < 0.05$ ) (Fig. 2A and B). This could be attributed to the increased aerosol concentration measured with the sampling probe inside the respirator. The increase occurred due to the airflow dynamics inside the respirator. With increasing inhalation flow rate, more aerosol particles penetrated inside the respirator per minute. The particles that passed through the leak followed the jet flow to the sampling probe, resulting in an increase in the aerosol concentration in the vicinity of the probe. The terminal velocity of the air jet flow at the sampling probe was estimated to be  $\sim 4.0 \text{ m s}^{-1}$  (the initial velocity of the jet flow at the leak outlet was  $20.4 \text{ m s}^{-1}$ ). This provided particles with sufficient inertial momentum to overcome the airflow initiated by the inhalation at  $40 \text{ l min}^{-1}$  (the air velocity at the inhalation inlet was  $1.3 \text{ m s}^{-1}$ ) so that the particles could reach the sampling probe. Thus, the protection factor decreased with increasing inhalation rate. This result supports the hypothesis that aerosol particles entering the

respirator through the face-seal leak are not homogeneously distributed in the respirator cavity.

In both cases ( $Q_{\text{INHALATION}} = 0$  and  $40 \text{ l min}^{-1}$ ), the particle size was found to significantly affect the protection factor ( $P < 0.05$ ). As seen in Fig. 2A and B, the protection factor increased with increasing particle size. This may be due to the impaction at the inlet of the leak (where the particles and airflow enter the leak), since the Stokes number increases with increasing particle size.

Figure 3A and B shows the effect of the depth of the sampling probe imbedded into the respirator as a function of particle size. At  $Q_{\text{TOTAL}} = 10 \text{ l min}^{-1}$ , there was no significant difference ( $P > 0.05$ ) in the protection factors obtained with the different depths of the sampling probe (Fig. 3A). Under these conditions, the leak flow was gentle so that it mixed well with the sampling flow regardless of the depth of the sampling probe inside the respirator. As the inhalation rate was increased from 0 to  $40 \text{ l min}^{-1}$ , the protection factors obtained with the sampling probe depths of 10 and 15 mm were significantly different ( $P < 0.05$ ) than those obtained with the depths of

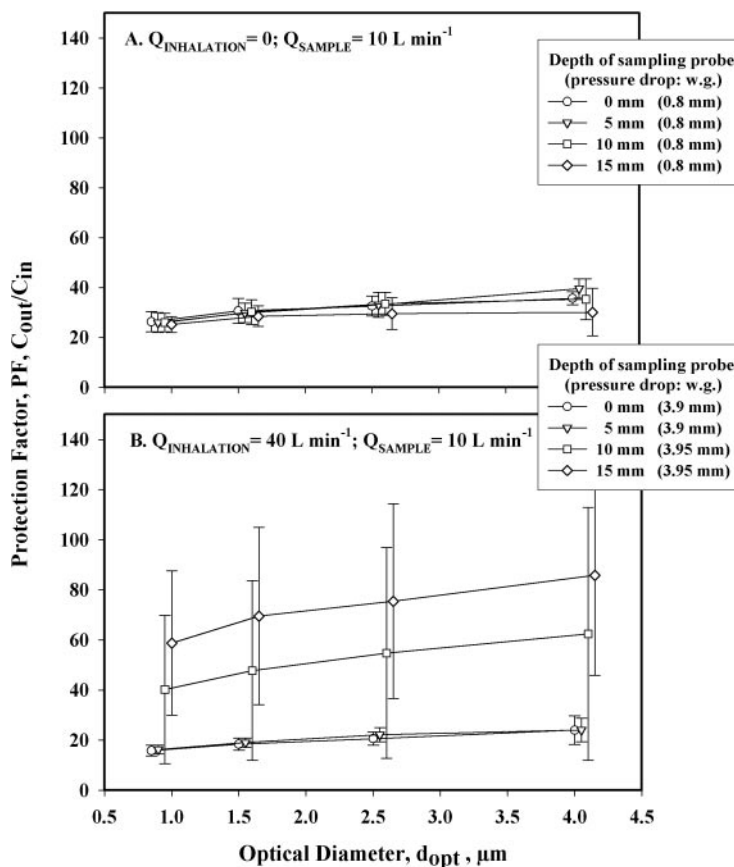
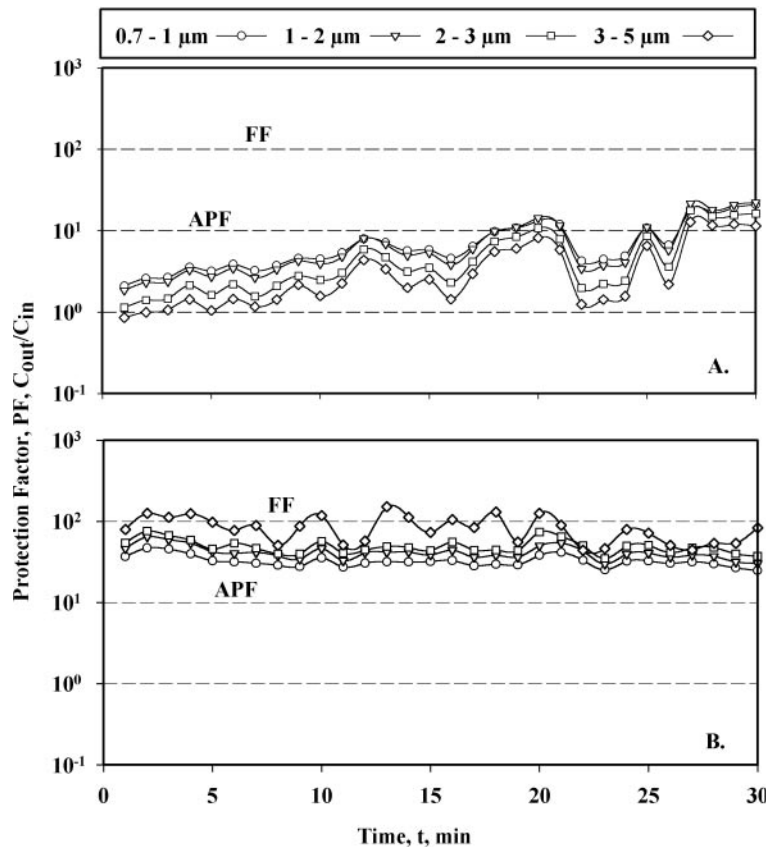


**Fig. 3.** Effect of the depth of the sampling probe on the protection factor at two inhalation flow rates: (A) 0 and (B)  $40 \text{ l min}^{-1}$ . The tests were performed using NaCl aerosol. The N95 respirator was fitted to the manikin's head. The leak location = chin; the leak cross section =  $1 \times 2 \text{ mm}^2$ . Each data point represents an average and standard deviation of three repeats. Each repeat was done with the same type of unused respirator.

0 and 5 mm. As shown in Fig. 3B, the protection factors increased when the depth of the sampling probe imbedded into the respirator increased. This indicates that the deeper the sampling probe, the lower the particle concentration measured with the sampling probe. As indicated earlier, the jet flow at a velocity of  $20.4 \text{ m s}^{-1}$  was directed toward the respirator filter and ended at the sampling probe inlet with a terminal velocity of  $4.0 \text{ m s}^{-1}$  (at a distance of 60 mm away from the leak outlet, where particles and airflow exit the leak into the respirator cavity). When the depth of the sampling probe increased, it is possible that the sampling flow did not mix well with the leak flow (because the aperture of the sampling flow decreased). It is anticipated that the jet airflow developed might not have been directed toward the sampling probe inlet but toward the respirator filter and the sampling probe body, resulting in particle losses due to inertial and turbulent deposition. In addition, as the depth of the sampling probe increased, the distance between the probe and the inhalation inlet ultimately decreased. For example, when the depth of the probe was 15 mm, this distance was as short as  $\sim 4 \text{ mm}$ , which is not sufficient for a smooth aerodynamic interaction. As a consequence,

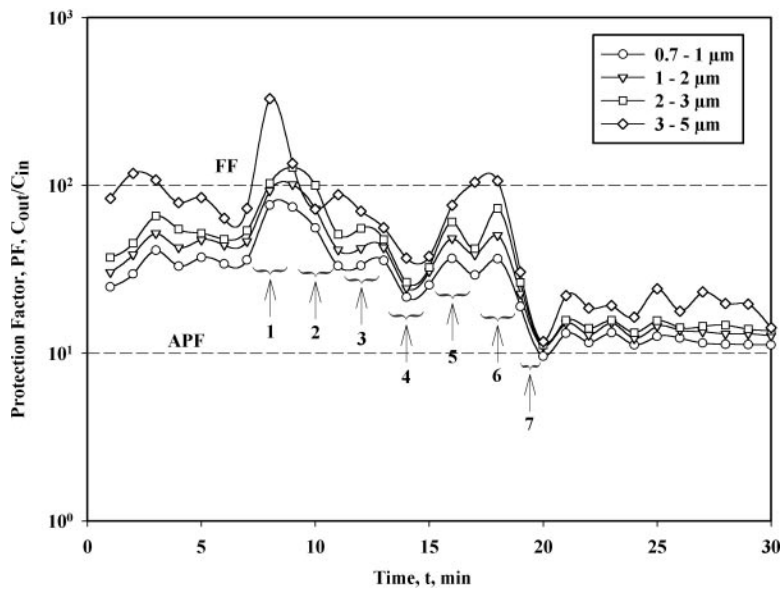
two competitive airflows (sampling and inhalation flows) might have caused an instability of the airflow around the sampling probe and resulted in particle losses inside the respirator. Thus, the greater depth of the probe led to an increase in the standard deviations of the protection factors as well as to a decrease in the aerosol concentrations measured with this probe inside the respirator. Based on these results, a small imbedding of the sampling probe (depth = 0–5 mm) is recommended for the in-facepiece aerosol sampling performed for the evaluation of the N95 filtering facepiece respirators.

Figure 4A and B present the protection factors for different particle sizes as a function of time. The data were obtained when a human subject, equipped with the personal setup, was exposed to NaCl aerosols while sitting and breathing normally in the center of the test chamber. Figure 5A shows the data obtained with no dryer installed in the in-facepiece sampling line, and Fig. 5B shows the results obtained with the dryer in the system. As seen from Fig. 5A, the protection factors varied with the particle sizes from 2 to 21 for  $d_{\text{opt}} = 0.7\text{--}1 \mu\text{m}$ , from 2 to 22 for  $d_{\text{opt}} = 1\text{--}2 \mu\text{m}$ , from 1 to 18 for  $d_{\text{opt}} = 2\text{--}3 \mu\text{m}$  and from 0.9 to 13 for  $d_{\text{opt}} = 3\text{--}5 \mu\text{m}$ . Thus, the protection factor



**Fig. 4.** Fractional protection factors measured on a human subject in the test chamber using NaCl aerosol without the dryer (A) and with the dryer (B). The subject breathed normally during the entire 30-min period. Each experiment was performed once. The same type of unused respirator was used in each experiment. FF = Fit Factor and APF = Assigned Protection Factor.





**Fig. 5.** The effect of the fit-testing exercise on the corresponding real-time respirator protection factor for a human subject exposed to NaCl aerosol. During all the other times the subject breathed normally. 1, deep breathing; 2, head side to side; 3, head up and down; 4, talking; 5, bend and touch the toes; 6, normal breathing; 7, grimace. The experiment was performed once. FF = Fit Factor and APF = Assigned Protection Factor.

decreased with increasing particle size. This finding contradicts the aerosol particle deposition model, which predicts lower penetration of large particles due to impaction and interception losses that occur when the aerosol passes through the leaks and the filter material. In addition, the protection factor at some time points was  $<1$ . Surprisingly, this indicates that the particle concentration inside the respirator was the same or higher than that outside the respirator. The calibration alarm was shown on the instrument display a few seconds after the measurement started. The data downloaded from the instrument data logger showed that the relative humidity was  $\sim 65$ – $87\%$  in the in-facepiece sampling line and  $\sim 12$ – $13\%$  in the ambient sampling line. The discrepancy between the results and the alarm status of the instrument was attributed to the high humidity of the air exhaled into the respirator cavity. In a high-humidity environment, the size of hygroscopic particles, such as NaCl, increases due to the absorption of water vapor, thereby increasing the concentration of larger particles and decreasing the concentration of smaller particles (Tang *et al.*, 1977). This increase in size can occur milliseconds after the particles have penetrated into the respirator cavity and may affect the measurement results in a different way outside and inside the respirator. Therefore, the protection factors obtained for smaller particles appeared to be greater than those for larger particles. In order to reduce the water content from the human-exhaled air, a dryer was designed and installed in the setup.

Once the system began operating with the dryer, the protection factors were always  $>1$  for particles in the

sizes ranging from  $0.7$  to  $5 \mu\text{m}$  as shown in Fig. 5B. Furthermore, the protection factor increased with increasing particle size. It varied from 25 to 47 for  $d_{\text{opt}} = 0.7$ – $1 \mu\text{m}$ , from 30 to 65 for  $d_{\text{opt}} = 1$ – $2 \mu\text{m}$ , from 37 to 76 for  $d_{\text{opt}} = 2$ – $3 \mu\text{m}$  and from 44 to 151 for  $d_{\text{opt}} = 3$ – $5 \mu\text{m}$ . The relative humidity was  $57$ – $68\%$  inside the respirator. Since the calibration alarm on the instrument screen never appeared, the dryer must have effectively removed water vapor from the exhaled air. Furthermore, the variability of the protection factor over a 30-min measurement period was reduced after the installation of the dryer. Initially, the coefficients of variance varied from 69.8 to 94.4% for  $d_{\text{opt}} = 0.7$ – $5 \mu\text{m}$ . After the dryer was installed, the coefficients of variance varied from 16.6 to 36.1%. The relative humidity and the variability of the measurement were reduced after the dryer was installed. Thus, our newly developed sampling system was ready for further human subject testing.

After the dryer was installed, the protection factor exceeded the APF (assigned protection factor) of 10 for all particle sizes, and was sometimes above the FF of 100 for larger particles. The FF and the APF are two different reference values used to evaluate the respiratory protection. With the quantitative fit test, an FF of 100 or above constitutes a pass. The FF is a quantitative estimate of the fit of a particular respirator to a specific individual when a respirator is worn under well-defined test conditions (US Department of Labor, 2003). In contrast, the APF is the level of the respiratory protection that a properly functioning respirator or class of respirators would be expected to provide to properly fitted and trained users in the

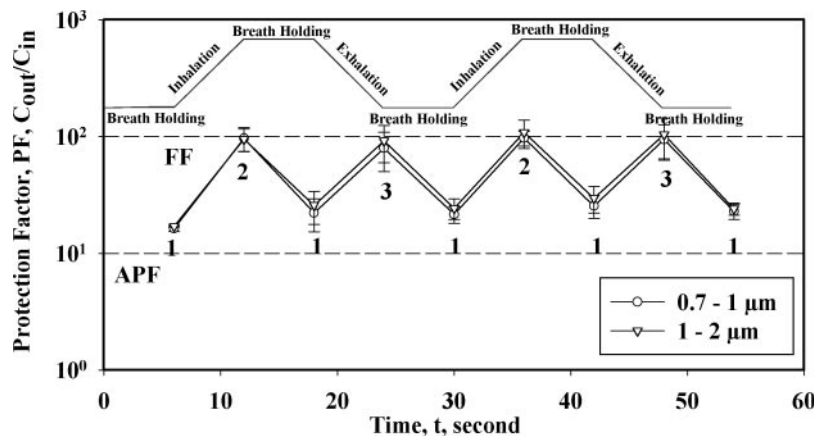
workplace (CDC, 1995; AIHARPC, 2002). The APF for filtering facepiece respirators is proposed to be 10 (US Department of Labor, 2003).

Figure 5 shows the effect of fit-testing exercises on the respirator protection factor. As seen, this sampling system can efficiently and immediately reflect the change in the protection factors due to different exercises. The results show that the protection factors for the talking exercise and the grimace exercise were lower than those for the other exercises. On the other hand, the protection factors were higher for the deep breathing maneuver. Crutchfield *et al.* (1999) also reported that FFs were the lowest for the talking exercise for the better-fitting respirators. This result can be explained by the increase in the aerosol concentration inside the respirator due to aerosolization of the particles generated from the mouth during the talking maneuver (Crutchfield *et al.*, 1993, 1995). The grimace maneuver, was designed to test the ability of the respirator to return to its original position, if an aggressive maneuver, such as smiling and frowning, disturbed the sealing surface. Thus, the protection factor usually decreases after the grimace maneuver. Deep breathing increased the protection factor because the increased leak flow might have caused particle losses in the leak and inside the respirator due to inertial and turbulent deposition. In addition, an increase in the inhalation flow during deep breathing may change the airflow aerodynamics in the respirator and cause more aerosol particles to be inhaled into the human respiratory tract instead of being sampled by the sampling probe, resulting in a higher protection factor.

Generally, the leaks created during the fit-testing exercises, except grimace, were transient, which suggested that the respirator fit was restored to the original level within 1 min after the exercises were

completed. As seen in Fig. 5, the protection factors at the time point of 7 min, which represented the normal breathing maneuver, were 34 for  $d_{opt} = 0.7\text{--}1\ \mu\text{m}$ , 44 for  $d_{opt} = 1\text{--}2\ \mu\text{m}$ , 48 for  $d_{opt} = 2\text{--}3\ \mu\text{m}$  and 64 for  $d_{opt} = 3\text{--}5\ \mu\text{m}$ . After all the exercises, excluding grimace, were completed and ended with the normal breathing maneuver, the respective protection factors were 37, 51, 73 and 107 (the time point of 18 min). Thus, the respirator regained about the same level of protection as it had during the first normal breathing maneuver. In contrast, when the grimace exercise was performed, the respirator fit decreased and could not be restored to the original level after the grimace maneuver ceased. As shown in Fig. 5, the protection factors after the grimace maneuver were 13 for  $d_{opt} = 0.7\text{--}1\ \mu\text{m}$ , 15 for  $d_{opt} = 1\text{--}2\ \mu\text{m}$ , 16 for  $d_{opt} = 2\text{--}3\ \mu\text{m}$  and 22 for  $d_{opt} = 3\text{--}5\ \mu\text{m}$ .

Figure 6 presents the change in the protection factors for different breathing patterns with a human subject: breath holding, inhalation and exhalation. Since the data were recorded with a 6-s averaging time, the particle concentrations inside the respirator were not sufficient for particles  $>2\ \mu\text{m}$ . Therefore, the protection factors for large particles are not presented in Fig. 6. As shown, the protection factors were lower during breath holding than during inhalation and exhalation, indicating that the particle concentration inside the respirator was greater when a subject held his breath. The breath holding resembles the laboratory testing conditions described above, when the manikin-based tests were conducted at  $Q_{INHALATION} = 0.1\ \text{min}^{-1}$  (Figs. 2A and 3A). The data presented in Fig. 2A ( $Q_{INHALATION} = 0.1\ \text{min}^{-1}$ ) were compared with those in Fig. 7A (human breath holding): the protection factors obtained with the manikin varied from 27 to 34 for  $d_{opt} = 0.7\text{--}2\ \mu\text{m}$ , while the protection factors obtained with the human



**Fig. 6.** Fractional protection factors measured in the test chamber during manipulated breathing patterns. The tests were conducted with a human subject exposed to NaCl aerosol. Each data point represents the average protection factor measured during the preceding 6 s, which is the average value and standard deviation of three repeats. In all the repeats, we used one respirator, which was not taken off between repeats. 1, holding breath; 2, inhalation; 3, exhalation. FF = Fit Factor and APF = Assigned Protection Factor.

subject varied from 16 to 30. Compared with only one circular leak artificially created between the manikin's face and the respirator, there should be many small leaks of different shapes around the face-seal area between the human face and the respirator. Oostenstad *et al.* (1990a, b) have reported that leaks may be circular or rectangular and there may be more than one leak on the wearer's face. Chen *et al.* (1992) have found that the leak flow decreased with an increase in complexity of the leak shape, which would also result in lower particle concentrations inside the respirator. In addition, small leak size leads to higher protection factors compared with large leak size because a small leak is more restrictive to the air flow. Therefore, the protection factor obtained for the human subject is the result of the summation of the protection factors contributed by the small leaks with different sizes and shapes around the human face-seal area.

During inhalation, the protection factor varied from 97 to 109 for  $d_{opt} = 0.7\text{--}2\ \mu\text{m}$  (Fig. 6). These protection factors are close to the value of 143 measured for  $d_{opt} = 0.7\text{--}2\ \mu\text{m}$  when the respirator was fully sealed on a manikin surface and the inhalation rate was  $40\ \text{l min}^{-1}$ . This indicates that most particles inside the respirators penetrated through the filter material into the respirator cavity during inhalation when a human subject had a good respirator fit. Due to the respiratory deposition of particles, the exhaled air contained few particles and diluted the particle concentration inside the respirator cavity. Thus, the protection factors were higher during exhalation than during breath holding. Wearing a respirator has a physiological effect on the wearer's breathing pattern. The breathing rate has been shown to increase when people put on a respirator regardless of the workload (Jones, 1991). Besides an increase in the respiratory rate (breaths per minute), the tidal volume

and the inspiratory time fraction of each respiration also increase when a respirator is donned (Hodous *et al.*, 1989). In addition, the respiratory deposition of particles has also been found to affect the measurement of the protection factor (Hewett *et al.*, 1993; Hinds *et al.*, 1993). These physiological factors may vary from one person to another and have a significant effect on the measurement of respiratory protection. In order to eliminate the confounding effect of individual variability, it is recommended that the breath holding maneuver, which can provide baseline information for the respirator fit, be included in the fit-test exercises.

When all the data collected during the different breathing patterns were combined in Fig. 6, the average protection factor was  $53 \pm 38$  for  $d_{opt} = 0.7\text{--}1\ \mu\text{m}$  and  $58 \pm 40$  for  $d_{opt} = 1\text{--}2\ \mu\text{m}$ . These results were compared with the protection factor values obtained with the same human subject during the normal breathing cycle. Figure 7 shows the protection factor data measured during normal breathing with the 6-s average over the period of  $\sim 10\ \text{min}$ . The protection factors averaged over the sampling periods were  $115 \pm 20$  for  $d_{opt} = 0.7\text{--}1\ \mu\text{m}$  and  $169 \pm 35$  for  $d_{opt} = 1\text{--}2\ \mu\text{m}$ . These results indicate that the mean was higher and the standard deviation was lower during the normal breathing cycle when compared with those obtained for the combined breathing patterns (breath holding, inhalation and exhalation) during the manipulated breathing cycle. During the normal breathing cycle, inhalation and exhalation lasted  $\sim 2\text{--}3\ \text{s}$  and the duration of the breath holding did not exceed 1 s, whereas each breathing pattern lasted 6 s during the manipulated breathing cycle. At such a short duration for the breath holding during the normal breathing cycle, the protection factor was relatively stable and mostly measured for inhalation and exhalation, which were associated with greater

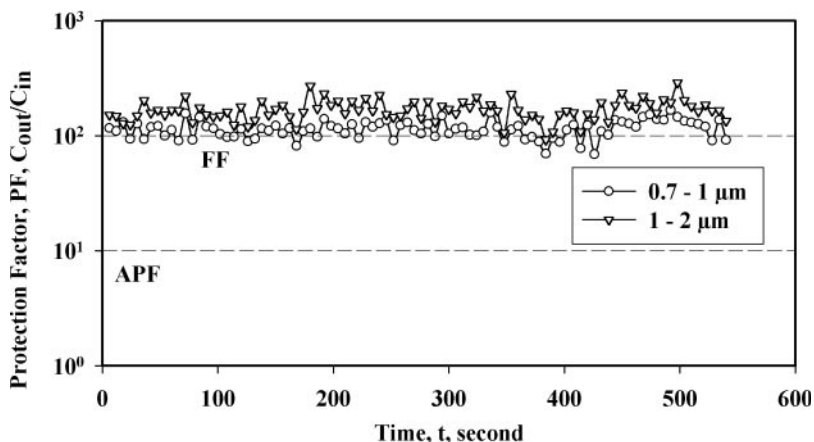


**Fig. 7.** Fractional protection factors measured every 6 s. The subject breathed normally while sitting in the test chamber during the entire time of the test. The tests were conducted with a human subject exposed to NaCl aerosol. The experiment was performed once with one respirator, which was not taken off between the repeated experiments as shown in Figs 6 and 7. FF = Fit Factor and AFP = Assigned Protection Factor.

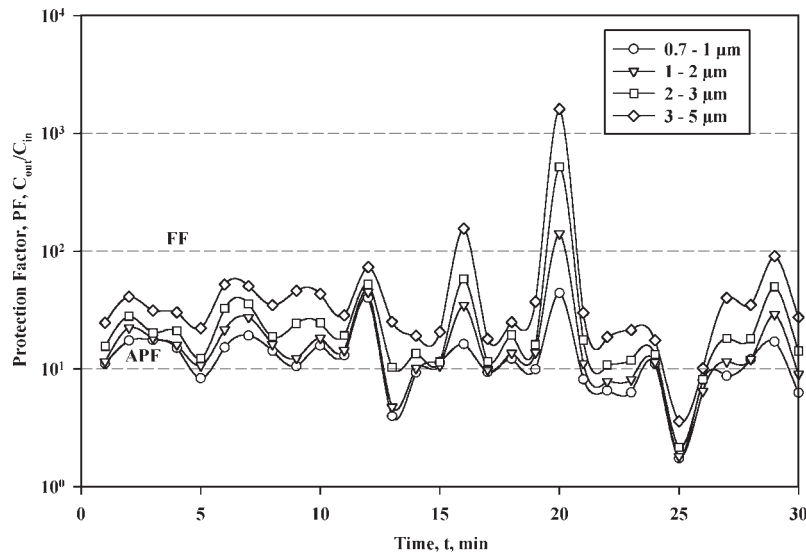


**Fig. 8.** Field testing on fractional protection factors during corn harvesting. The subject breathed normally and stood on the combine, outside the cockpit, during the entire 30-min period. FF = Fit Factor and APF = Assigned Protection Factor.

protection factors than the breath holding. In addition, the particle concentrations inside the respirator were usually not sufficient to calculate the protection factors in a timescale as short as 6 s, especially for large particles and moderately contaminated environments. In field applications, increasing the sampling time is important to collect representative data.

Figure 8 presents the results of field measurements conducted during corn harvesting. The protection factors over the period of 30 min with the 1-min average varied from 2 to 44 for  $d_{opt} = 0.7\text{--}1\ \mu\text{m}$ , from 2 to 141 for  $d_{opt} = 1\text{--}2\ \mu\text{m}$ , from 2 to 519 for  $d_{opt} = 2\text{--}3\ \mu\text{m}$  and from 4 to 1611 for  $d_{opt} = 3\text{--}5\ \mu\text{m}$ . The field data were lower and more variable than to the laboratory data shown in Fig. 5. The field results demonstrate that this sampling system can be successfully used in real situations.

## CONCLUSIONS

The newly developed sampling system for measuring the protection provided by the N95 filtering facepiece respirators against particles has demonstrated its ability to successfully assess the effects of face seal characteristics, human activity and breathing patterns on the protection factors when the sampling probe was imbedded on the respirator surface (the imbedded depth = 0 mm). This sampling system can efficiently detect changes in the in-facepiece and ambient aerosol concentrations in real time every 6 s for the particle size range of  $0.7\text{--}2\ \mu\text{m}$ . Therefore, this sampling system is capable of determining the protection factors against particles in the above size range for different breathing patterns within a short time. In addition, increasing the sampling time from 6 s to 1 min allowed the collection of a sufficient number of

particles to assess the protection factors against particles in the size range of  $0.7\text{--}5\ \mu\text{m}$  in both laboratory and field studies.

*Acknowledgement*—This study was supported by the National Institute for Occupational Safety and Health through grant no. RO1-OH-04085.

## REFERENCES

- ACGIH. (1998) Industrial ventilation: a manual of recommended practice, 23rd edn. Cincinnati, OH: American Conference of Governmental Industrial Hygienists. ISBN 1 882417 22 4.
- American Industrial Hygiene Association Respiratory Protection Committee. (2002) Respirator performance terminology (Letter to the editor). *Am Ind Hyg Assoc J*; 63: 130, 132.
- ASHRAE. (1997) ASHRAE Handbook Fundamentals, IP Edition. Atlanta, GA: American Society of Heating, Refrigerating and Air-Conditioning Engineers, Inc. pp. 31.1–31.17. ISBN 1 883413 44 3.
- Baron PA, Willeke K. (2001) Sampling and transport of aerosol. In: Baron PA, Willeke K, editors. *Aerosol Measurement: Principles, Techniques, and Applications*, 2nd edn. New York: Wiley-Interscience. pp. 61–82. ISBN 0 471 35636 0.
- Brazile WJ, Buchan RM, Sandfort DR, Melvin W, Johnson JA, Charney M. (1998) Respirator fit and facial dimensions of two minority groups. *Appl Occup Environ Hyg*; 13: 233–7.
- CDC, NIOSH. (1995) 42 CFR 84 Respiratory Protective Devices; Final Rules and Notice. Federal Register 60:110. Cincinnati, OH: Centers for Disease Control and Prevention, National Institute for Occupational Safety and Health.
- Chen CC, Willeke K. (1992) Characteristics of face seal leakage in filtering facepieces. *Am Ind Hyg Assoc J*; 53: 533–9.
- Chen CC, Ruuskanen J, Pilacinski W, Willeke K. (1990) Filter and leak penetration characteristics of a dust and mist filtering facepiece. *Am Ind Hyg Assoc J*; 51: 632–9.
- Choe K, Trunov M, Grinshpun SA, *et al.* (2000) Particle settling after lead-based paint abatement work and clearance waiting period. *Am Ind Hyg Assoc J*; 61: 798–807.
- Coffey CC, Campbell DL, Myers WR, Zhuang Z. (1998) Comparison of six respirator fit-test methods with an

- actual measurement of exposure in a simulated health care environment: Part II—Method comparison testing. *Am Ind Hyg Assoc J*; 59: 862–70.
- Crutchfield CD, Park DL. (1997) Effect of leak location on measured respirator fit. *Am Ind Hyg Assoc J*; 58: 413–7.
- Crutchfield CD, Van Ert M. (1993) An examination of issues affecting the current state of quantitative respirator fit testing. *J Int Soc Resp Prot*; 11: 5–18.
- Crutchfield CD, Park DL, Hensel JL *et al.* (1995) Determinations of known respirator leakage using controlled negative pressure and ambient aerosol QNFT systems. *Am Ind Hyg Assoc J*; 56: 16–23.
- Crutchfield CD, Fairbank EO, Greenstein SL. (1999) Effect of test exercises and mask donning on measured respirator fit. *Appl Occup Environ Hyg*; 14: 827–37.
- Day DE, Malm WC, Kreidenweis SM. (2000) Aerosol light scattering measurements as a function of relative humidity. *J Air Manag Assoc*; 50: 710–6.
- Grinshpun SA, Adhikari A, Lee BU *et al.* (2004) Indoor air pollution control through ionization. In: *Air Pollution: Modeling, Monitoring, and Management of Air Pollution* ed. C.A.Brebba. WIT Press, Southampton, UK, pp. 689–704.
- Hewett P, Pally BG, Gamble JF. (1993) A model for correcting workplace protection factors for lung deposition and other effects. *Am Ind Hyg Assoc J*; 54: 142–9.
- Hinds WC, Bellin P. (1993) The effect of respirator dead space and lung retention on exposure estimates. *Am Ind Hyg Assoc J*; 54: 711–22.
- Hodous TK, Hankinson JL, Stark GP. (1989) Workplace measurement of respirator effects using respiratory inductive plethysmography. *Am Ind Hyg Assoc J*; 50: 372–8.
- Holton PM, Tachett DL, Willeke K. (1987) Particle size dependent leakage and losses of aerosols in respirators. *Am Ind Hyg Assoc J*; 48: 848–54.
- ICRP (International Commission on Radiological Protection). (1994) Human respiratory tract model for radiological protection, ICRP publication 66. *Ann ICRP*; 24(1–3).
- Jones JG. (1991) The physiological cost of wearing a disposable respirator. *Am Ind Hyg Assoc J*; 52: 219–25.
- Lee SA, Reponen T, Li W *et al.* (2004) Development of a new method for measuring the protection provided by respirators against dust and microorganisms. *Aerosol Air Quality Res*; 4: 55–72.
- Liu BYH, Segal K, Rubow KL *et al.* (1984) In-mask aerosol sampling for powered air purifying respirators. *Am Ind Hyg Assoc J*; 45: 278–83.
- Myers WR, Allender JR, Iskander W *et al.* (1988) Causes of in-facepiece sampling bias—I. Half-facepiece respirators. *Ann Occup Hyg*; 32: 345–59.
- Nelson TJ, Colton CE. (2000) The effect of inhalation resistance on facepiece leakage. *Am Ind Hyg Assoc J*; 61: 102–5.
- Oestenstad RK, Perkins JL, Rose VE. (1990a) Identification of faceseal leak sites on a half-mask respirator. *Am Ind Hyg Assoc J*; 51: 280–4.
- Oestenstad RK, Dillon HK, Perkins LL. (1990b) Distribution of faceseal leak sites on a half-mask respirator and their association with facial dimensions. *Am Ind Hyg Assoc J*; 51: 285–90.
- Ojanen J, Mikkanen P, Martuzevicius D, *et al.* (2004) Continuous mass size distribution measurement and drying of urban PM<sub>2.5</sub> particles. In: *Sustainable Development—Proceedings of the 97th Annual Conference of Air & Waste Management Associations* AWMA Press, Indianapolis, IN, USA: VIP-127-CD: 201.1–201.14.
- OSHA. (1998) Respiratory Protection: 29 CFR 1910.134, Appendix A. Washington, DC: US Department of Labor, Occupational Safety and Health Administration.
- OSHA. (2003) 29 CFR Parts 1910, 1915, and 1926 Assigned Protection Factors; Proposed Rule- 68:34035-34119. Federal Register/ Vol. 68, No. 109. Washington, DC: US Department of Labor, Occupational Safety and Health Administration.
- Qian Y, Willeke K, Grinshpun S *et al.* (1998) Performance of N95 respirators: filtration efficiency for airborne microbial and inert particles. *Am Ind Hyg Assoc J*; 59: 128–32.
- Tang IN, Munkelwitz HR, Davis JG. (1977) Aerosol growth studies—II. Preparation and growth measurements of monodisperse salt aerosols. *J Aerosol Sci*; 8: 149–59.
- Willeke K, Qian Y, Donnelly J *et al.* (1996) Penetration of airborne microorganisms through a surgical mask and dust/mist respirator. *Am Ind Hyg Assoc J*; 57: 348–55.